Journal of Insect Physiology 57 (2011) 372–384

Contents lists available at ScienceDirect

Journal of Insect Physiology

journal homepage: www.elsevier.com/locate/jinsphys

Honeybee (*Apis mellifera ligustica*) drone embryo proteomes

Jianke Li, Yu Fang *, Lan Zhang, Desalegn Begna

Institute of Apicultural Research, Chinese Academy of Agricultural Science/Key Laboratory of Pollinating Insect Biology, 1# Beigou, Xiangshan, Haidian District, Beijing 100093, China

ARTICLE INFO

Article history:
Received 2 November 2010
Received in revised form 9 December 2010
Accepted 10 December 2010
Available online 21 December 2010

Keywords:
Honeybee
Drone
Embryo
2-DE
MALDI-TOF/MS
LC-Chip/ESI-QTOF

ABSTRACT

Little attention has been paid to the drone honeybee (*Apis mellifera ligustica*) which is a haploid individual carrying only the set of alleles that it inherits from its mother. Molecular mechanisms underlying drone embryogenesis are poorly understood. This study evaluated protein expression profiles of drone embryogenesis at embryonic ages of 24, 48 and 72 h. More than 100 reproducible proteins were analyzed by mass spectrometry on 2D electrophoresis gels. Sixty-two proteins were significantly changed at the selected three experimental age points. Expression of the metabolic energy requirement-related protein peaked at the embryonic age of 48 h, whereas development and metabolizing amino acid-related proteins expressed optimally at 72 h. Cytoskeleton, protein folding and antioxidant-related proteins were highly expressed at 48 and 72 h. Protein networks of the identified proteins were constructed and protein expressions were validated at the transcription level. This first proteomic study of drone embryogenesis in the honeybee may provide geneticists an exact timetable and candidate protein outline for further manipulations of drone stem cells.

1. Background

In the honeybee society, female workers are the dominant sex. Male drones are mainly present during the mating season when their main function is limited to mating with the virgin queen. Male drones never exhibit typical worker bee behaviors such as collecting nectar, pollen brood nursing and nest construction (Klenk et al., 2004). As an evolutionary consequence to conserve food, workers expel drones out of the hive when the colonies are preparing for winter (Winston, 1987). Drones are haploid and being derived through parthenogenesis from unfertilized eggs laid by the queen. Thus they inherit just one set of chromosome from their mother. This enables the honeybee to adapt to stress factors through the haploidy–diploidy mechanism of sex determination (Beye et al., 2003). The genotype of the drone is not complicated by the presence of dominant and recessive alleles as in the case of diploid queens and workers (Javier et al., 1991). Accordingly, genes of drones are effectively homozygous at any locus (Javier et al., 1991). Drones are a potentially powerful selection tool for the genetic improvement of the honeybee as they genetically contribute equally with the queen so that the egg develops into either a queen or worker. Manipulation of drone embryos at the molecular level could produce ideal offspring to facilitate more honey or royal jelly production to satisfy human demand.

Honeybee embryogenesis undergoes ten developmental stages (Fleig and Sander, 1986). During ontogenesis genetic materials can be introduced into the young egg (Amdam et al., 2003; Dearden, 2006). Honeybee workers have been successfully obtained from transgenic embryos (Aase et al., 2005). There is no doubt that unraveling the global biochemical and physiological mechanisms involved in the complex developmental process at the functional molecular level is a prerequisite for gene manipulation. Proteomic analysis of honeybee, larval development (Chan and Foster, 2008; Li et al., 2007), hypopharyngeal gland development (Feng et al., 2009) and spermathecal fluid (Baer et al., 2009) have been performed. These studies have laid the foundation for revealing drone embryogenesis and have helped us obtain a deeper insight into honeybee biology at the protein level. Since drones play critical roles in honeybee breeding, it is indispensable to perform the proteomic analysis of drone embryogenesis. The recently announced decoding of the honeybee genome (Sequencing Consortium, 2006) enables us to study honeybee gene expression in a global proteomic approach. This present study was conducted to systemically analyze protein expression profiles during drone embryonic development and provide basic information for future manipulation of male embryonic stem cells to breed honeybee that produce increased amounts of royal jelly and honey.

* Corresponding author. Tel.: +86 10 62591449; fax: +86 10 62591449.
E-mail addresses: apislijk@126.com (J. Li), freky@163.com (Y. Fang), lovebabycyndi@126.com (L. Zhang), desalegnbegna@yahoo.co.uk (D. Begna).

0022-1910/$ – see front matter. Crown Copyright © 2010 Published by Elsevier Ltd. All rights reserved.
doi:10.1016/j.jinsphys.2010.12.007

2. Materials and methods

2.1. Chemical regents

Urea, Tris-base, sodium dodecyl sulfate (SDS), sodium bicarbonate (NH_4HCO_3), dithiothreitol (DTT), iodoacetamide and bovine serum albumin (BSA) were purchased from Sigma (St. Louis, MO, USA). Bio-lyte from Bio-Rad (Hercules, CA, USA), acrylamide, N,N′-methylenebisacrylamide, ammonium persulfate (APS), N,N,N′,N′-tetramethylethylene diamine (TEMED), 3-[(3-cholamidopropyl)-dimethylammonio]-1-propane sulfonate (CHAPS), glycerol, bromophenol blue, coomassie brilliant blue (CBB) G-250. α-Cyano-4-hydroxycinnamic acid (CHCA) from Bruker Daltonics (Billerica, MA, USA), trypsin from Roche (Modified, Sequencing Grade, Roche, Mannheim, Germany), and trifluoroacetic acid (TFA) and acetonitrile from J. T. Baker (Phillipsburg, NJ, USA). All the chemicals used for RNA isolation and real-time PCR were from Bio-Rad (Hercules, CA, USA). While, other chemicals used but not specified here were noted with their sources in the text.

2.2. Biological samples

Mated queen bees (*A. m. ligustica*) were imported from Bologna, Italy in May 2009. The queens were introduced into honeybee colonies at the Institute of Apicultural Research, Chinese Academy of Agricultural Science. In order to precisely determine the age of the eggs, the queens were confined and provided with empty drone combs and left undisturbed for 5 h to lay eggs. The queen was removed and the combs containing drone eggs was placed in an area where queen access was forbidden. Drone eggs at 24, 48 and 72-h after releasing the queen were collected (1000 eggs as one biological sample for each time point) using a plastic honeybee egg transferring tool from May to July, 2009.

2.3. Protein extraction and two-dimensional gel electrophoresis (2-DE)

Drone eggs were mixed in phosphate-buffered saline (PBS, 1 mg/10 μl). The mixture was homogenized for 5 min on ice and sonicated for 2 min. The mixture was centrifuged at 12,000 × *g* for 10 min at 4 °C and re-centrifuged at 15,000 × *g*. The supernatant was collected and the pellet was resuspended in PBS (1 mg/2 μl) and centrifuged at 15,000 × *g* for 10 min at 4 °C and again, the supernatant was collected and pooled with the first collection. This specimen was referred to as PBS-soluble drone egg protein extract. The pellet containing PBS-insoluble proteins was mixed in a lysis buffer (LB, 8 M urea, 2 M thiourea, 4% CHAPS, 20 mM Tris-base, 30 mM DTT, 2% Bio-lyte pH 3–10, 1 mg/10 μl). The lysate was sonicated for 2 min and centrifuged at 15,000 × *g* for 10 min at 4 °C. The supernatant was collected and mixed with PBS-soluble proteins extract. Trichloroacetic acid was added to the samples constituting 10% of the final volume of the supernatant. The sample was kept on ice for 10 min to allow protein precipitation and desalting. Subsequently, the sample was centrifuged twice at 15,000 × *g* for 10 min at 4 °C. The supernatant was discarded and the pellet was re-suspended in LB (1 mg/4 μl). The sample was homogenized for 5 min on ice and sonicated for 2 min. The pH of the samples was adjusted to 7.0 with 2 M NaOH and the protein concentration was determined according to Bradford (Bradford, 1976).

The above protein sample (280 μg) was suspended in 84 μl LB and mixed with 336 μl rehydration buffer (8 M urea, 2% CHAPS, 0.001% bromophenol blue, 45 mM DTT, 0.2% Bio-lyte pH 3–10). The mixture was loaded onto a 17 cm IPG strip (immobilized pH gradient, pH 3–10, linear, Bio-Rad). Isoelectric focusing (IEF) was performed (Protean IEF Cell, Bio-Rad) at 18 °C according to the following program: 14 h at 50 V; 250 V for 30 min × 4 times; 1000 V for 60 min; 9000 V for 5 h; 9000 V, for 60,000 Vh. Prior to SDS-PAGE (sodium dodecyl sulfate polyacrylamide gel electrophoresis), the IPG strips were first equilibrated for 15 min in equilibration buffer 1 (6 M urea, 0.375 M Tris–HCl pH 8.8, 20% glycerol, 2% SDS, 2% DTT) and later in equilibration buffer 2 (6 M urea, 0.375 M Tris–HCl pH 8.8, 20% glycerol, 2% SDS, 2.5% iodoacetoamide) for 15 min. After equilibration, the strip was transferred to SDS polyacrylamide gel, 12% T separating gel (1.00 mm). Second dimension electrophoresis, SDS-PAGE, was performed in a Protean II Xi Cell (Bio-Rad) at 25 mA/gel for 6 h. The gels were fixed overnight in 50% (v/v) ethanol with 10% (v/v) acetic acid, washed in water, and stained with CBB G-250. The best three runs with good reproducibility from triplicated samples were subjected to PDQuest V 8.0 (Bio-Rad) analysis. The authenticity and outline of each spot were validated by visual inspection and edited when necessary.

2.4. Image acquisition and statistics analysis

For comparison, each spot volume was normalized against total spot volume obtained from triplicated samples. The matched sets were created for all samples and a quantitative table with normalized optical spot volumes was generated to allow analysis of variance (ANOVA, Version 6.12, SAS Institute) Duncan parametric test. An error probability of $p < 0.05$ was considered to be statistically significant when applying 1.5 fold changes.

2.5. Trypsinization for mass spectrometry

The CBB stained spots were manually excised in triplicate gels from each developmental stage and destained for 30 min using 100 ml acetonitrile (50%) and 25 mM NH_4HCO_3 pH 8 (50%) for three to four times until gels were transparent. The gels were dehydrated for 10 min with acetonitrile (100%) and dried for 30 min using a Speed-Vac system. To prepare trypsin solution, 2.5 ml of 25 mM NH_4HCO_3 was added to 25 μg trypsin (final concentration 10 ng/μl, Roche). The trypsin solution (10 μl) was pipetted onto each dried protein spot and incubated for 60 min at 4 °C. To avoid trypsin autodigestion, the excessive trypsin was removed. Then the sample was incubated for 14 h at 37 °C. To extract the peptide fragments from the tryptic digests, 20 μl of 5% (v/v) TFA were added and incubated for 60 min at 37 °C. Thereafter, 20 μl of 50% (v/v) acetonitrile [containing 2.5% (v/v) TFA] acid were added to gel pieces and incubated for 60 min at 30 °C. After each step, the supernatants were pooled and dried using a Speed-Vac system.

2.6. Protein identification by mass spectrometry

Matrix was prepared by dissolving CHCA in 50% acetonitrile/0.1% trifluoroacetic acid. Ten microliters of solution was added onto the dried digests and vortexed for 30 min. A total of 1.5 μl of the reconstituted in-gel digest sample was spotted initially on Anchorchip target plate (600/384F, Bruker Daltonics), followed by adding 1 μl of matrix solution. The dried sample on the target was washed twice with 1 μl 0.1 TFA and left for 30 s before solvent removal. Mass spectra were acquired on an Ultraflex MALDI TOF-TOF/MS (matrix assisted laser desorption ionization time of flight/mass spectrometry, Bruker Daltonics) in reflectron, positive mode in the mass range of 700–4000 Da. Spectra were calibrated by a protonated mass signal from a standard peptide calibration mixture consisting of eight peptides covering mass range from 700 to 3100 Da for MALDI-TOF/MS. MS spectra were analyzed with flexAnalysis (version 2.2, Bruker Daltonics) using parameter as signal/noise threshold >6, resolution >1500, and centroid algorithm for monoisotopic peak assignment. All known contaminants (trypsin autoproteolysis and known keratin peaks) were excluded during the process. The measured tryptic peptide masses were

transferred through BioTool (Version 2.2, Bruker Daltonics) as inputs to search against the nonredundant database of national center for biotechnology information (NCBInr, release date, June 26, 2008) using MASCOT 2.2 (Matrix Science). Search parameters were: taxonomy: all entries; trypsin cleavage; allow up to one missed cleavage; peptide mass tolerance 0.2 Da; fixed modification: carbamidomethyl (C); variable modification: oxidation (M). A total of 6,649,798 sequences and 2,279,950,795 residues in the database were actually searched.

Protein with lower abundance that could not be identified by MALDI-TOF/MS was identified by liquid chromatography-chip/electrospray ionization-quadruple time-of-flight/mass spectrometry (LC-Chip/ESI-QTOF-MS) (QTOF G6530, Agilent Technologies), equipped with a capillary pump G1382A, a nano pump G2225A, an autosampler G1377D and the Chip Cube G4240A. The LC-Chip used (Agilent Technologies) was constituted of a Zorbax 300SB-C18 enrichment column (40 nl, 5 μm) and a Zorbax 300SB-C18 analytical column (75 μm × 43 mm, 5 μm). The loading flow rate was 4 μl/min and the loading mobile phase was water with 0.1% formic acid. Elution from the analytical column was performed by a binary solvent mixture composed of water with 0.1% formic acid (solvent A) and acetonitrile with 0.1% formic acid (solvent B). The following gradient program was used: from 3% to 8% B in 1 min, from 8% to 40% B in 5 min, from 40% to 85% B in 1 min and 85% B for 1 min. The chip flow rate was 300 nl/min. The MS conditions were: positive ion mode; Vcap: 1900 V; drying gas flow rate: 5 l/min; drying gas temperature: 350 °C; fragment voltage: 175 V; skimmer voltage: 65 V; reference masses: *m/z* 149.02332 and 1221.02332. The digested samples were diluted in 20 μl water with 0.1% formic acid; centrifuged for 5 min at 10,000 × *g* and about 15 μl of upper solution was analyzed and used to inject 8 μl of sample for analysis. Spectra were calibrated by mass reference standard purine and HP-0921 (121. 050873, 922.009798, Agilent Technologies). Tandem mass spectra were retrieved using the MassHunter software (Version B. 02. 01, Agilent Technologies). Before MS/MS data searching, peak-list was generated by Mascot Distiller software (Version 3.2.1.0, Matrix Science). MS/MS data were searched against Mascot 2.2 (Matrix Science) applied to NCBInr (release date, June 26, 2008). Search parameters: carboxymethyl (C) and oxidation (M) were selected as variable modifications and no fixed modification was selected. The other parameters used were: taxonomy: all entries; enzyme: trypsin; missed cleavages: 1; peptide tolerance: ±1.2 Da, MS/MS tolerance: ±0.6 Da. A total of 6,649,798 sequences and 2,279,950,795 residues in the database were actually searched.

When the identified peptides matched to multiple members of a protein family, or a protein appeared under the same names and accession number, the match was made in terms of higher Mascot score, the putative function and differential patterns of protein spots on 2-DE gels. Protein identification were accepted if they establish probability greater than 95% and contained at least 2 identified peptides having maximum peptide coverage.

2.7. Protein classification and hierarchical cluster analysis

The identified proteins were searched against the Uniprot database. Combined with the results obtained from Flybase search, the proteins were grouped based on their biochemical functions. Hierarchical cluster of the expression profiles was performed by the expression values of protein spots at different developmental time point by average software calculated distance using cluster software (Gene cluster, Version 3.0).

2.8. Quantitative real-time PCR

Total RNA was extracted from 24, 48 and 72-h old drone embryos using TRIzol regent (Takara bio). Reverse transcription was performed using a RNA PCR Kit (Takara bio), according to the manufacturer's instructions. Thirteen differentially expressed proteins from four major functional groups (carbohydrate metabolism and energy production, protein folding, development and antioxidant) were selected for qRT-PCR analysis and glyceraldehyde-3-phosphate dehydrogenase (GAPDH) was used as the reference (Table 1). Real-time PCR was conducted using an iQ5 Multicolor Real-Time PCR Detection System (Bio-Rad). PCR was performed in 25-μl reaction system containing 1 μl cDNA, 5 pmol forward and reverse primers, 12.5 μl SYBR Green Supermix (Bio-Rad) and water. Fold-change was calculated using $2^{-\Delta\Delta Ct}$ method (Livak and Schmittgen, 2001). Each sample was analyzed independently and processed in triplicate. The values from the 3 independently obtained results were analyzed using ANOVA and means compared using Duncan's Parametric Test (SAS, Version 6.12, SAS Institute). An error probability $p < 0.05$ was considered statistically significant.

2.9. Biological network analysis

To predict protein–protein interaction, the identified drone embryo proteins were analyzed by Pathway Studio software (Ariadne Genomics). Briefly, the protein list was run against the *Drosophila* database that was equipped with functional relationships from other scientific literature. The filters that we applied included "all shortest paths between selected entities". The information received was narrowed down to our proteins of interest. Each link was built based on evidence from at least three publications. Different symbols were employed by the software to define proteins, i.e., "red elipse" for proteins, "sickle" for kinases, "rhomb" for ligands, "stick" for receptors, "O-vertex" for transcription factors, "2 triangles" for phosphates, "sticks" for receptors, "grey elipse" for cell objects, "orange hexapon" and "yellow rectangle" for cell process.

3. Results

3.1. Protein profiling of drone eggs at different developmental stages of embryogenesis

Quantitative and qualitative images of honeybee drone embryogenesis samples from three embryonic age points (24, 48 and 72 h) were analyzed using 2-DE. Accordingly, 283 ± 18, 305 ± 20 and 293 ± 13 protein spots were detected. Of the total detected protein spots, 102, 103 and 104 proteins were successfully analyzed by MS, respectively (Fig. 1). Sixty-two protein spots were significantly altered across three embryonic age points ($p < 0.05$) when applying a threshold of a 1.5 fold-change (Table 2). Likewise, 45 proteins with no significant differential expression were used to build a reference proteome map (Table 3). Some proteins spots were unable to be identified. This may be caused by a protein level too low to produce sufficient spectrums, or database search scores not higher than 95% which would yield unambiguous results.

Proteins identified at three embryonic ages were classified into nine functional categories based on their biological activity. The most represented categories were proteins related to carbohydrate metabolism and energy production (27%), followed by a group of proteins with folding function (21%). Heat shock proteins (Hsp) represented the majority in this group. The third largest protein family was development associated proteins (16%). The other proteins were involved in antioxidant activity (9%), the cytoskeleton (8%), translation and transcription function (7%), amino acid metabolism (7%), nucleic acid metabolism (3%) and proteins with unknown function (2%) (Fig. 2A). Regarding the classification of the 45 proteins that exhibited stable expression, proteins involved in carbohydrate

Table 1
Primer sequences used for validating real-time PCR of genes differential expressed during the embryonic development of honeybee drone (*Apis mellifera* L.).

Spot number	Accession number	Protein name	Primer: sense 5′–3′, antisense 5′–3′	Product size	Annealing temperature
A11	gi|66531851	Protein disulfide-isomerase precursor	CAATGAGTATGGAGTAGAAGATGG CAACAACTAATGGCAGTGAATG	134	59.0
B31	gi|66549336	Ubiquitin-like protein smt3	TGGCAATAGCAGCAGTAAGG ATTTCAAGAGTAGTTGGTGTATCC	76	59.0
B33	gi|66547447	ATP phosphohydrolase	GACCTGGACAAAGAAATGATAAAG TTCTACCTTAGTTCCACCATATTC	98	59.0
A29	gi|48104167	Nuclear transport factor-2	GATCCACCACATGCCTTCTC ATGAATGCCAAGACGAAAGATG	93	59.0
A28	gi|66534766	Cytochrome-c oxidase	GGCATGGTTATGTAGTCGTATTG TCCCGTAGCAAGTTCCAATG	115	59.0
A24	gi|66515987	Translationally-controlled tumor protein homolog	GGTGAATCTATGGACATTGATGG TGCTTGAATAACATGAGAACAGG	92	59.0
A21	gi|66534655	Glutathione S transferase S1	AAGTGAAGAATAATGGTGGCTAC CAGAATGTGGACGCTTATCAAG	198	59.0
A14	gi|66552230	26S proteasome non-ATPase regulatory subunit 14	AAGCCATCTGTTCAAGCATTG TCAGCAAGTGTAAGACCATCC	143	59.0
A9	gi|66558942	T-complex protein 1 delta subunit	ATTCTTCGTGATGCTGTTAGTG ATCTAATGATGCGATTGGTCTG	138	59.0
B11	gi|48095525	Tubulin β-1 chain	GGTATGGACGAGATGGAGTTC GCCTCTTGGTATTGCTGATATTC	80	59.0
A27	gi|66520497	Nucleoside diphosphate kinase	ATTATGATTAAGCCTGATGGTGTC GGTACAACTGGTCCTGAACTC	200	59.0
A10	gi|66521545	Tubulin α-1 chain	TGTTATCCAATACTACTGCTATCG CCAACCTCTTCATAATCCTTCTC	178	59.0
A4	gi|66540596	T-complex protein 1 eta	TGATGCTATAATGGTTGTAAGACG CCTGCTATCACACGAGAATAATC	148	59.0

Spot number corresponds to the number of protein spots in Fig. 2A and Table 2. Accession number and protein name are correspond to the differentially identified proteins in Table 2.

metabolism and energy production, proteins folding, developmental processes and antioxidants comprised the top four groups (Fig. 2B).

3.2. Cluster expression analysis of the identified proteins

The protein expression pattern at three embryonic differentiation stages was further analyzed using hierarchical clusters. The clustering showed that 62 differentially expressed protein spots across the ages behaved heterogeneously (Fig. 3). Only a few (nine) up-regulated proteins were identified at 24 h. Four (spots B13, B14, B25 and B17) of them were related to carbohydrate metabolism and energy production. Two (spots B5, B9) were involving in protein folding. The other three (spot B18, spots B3 and B24) were associated with developmental regulation, the cytoskeleton and fatty acid metabolism (Fig. 3).

At the 48 h embryonic stage, 28 proteins were highly expressed and similar to the 24 h period, the largest protein family (11 proteins) was involved in carbohydrate metabolism and energy production (spots A16, B12, B22, B23, B10, B16, B19, B26, B29, B20 and B33). The second largest protein family contained seven proteins (spots A2, A6, B1, B2, B4, B6 and B7) associated with

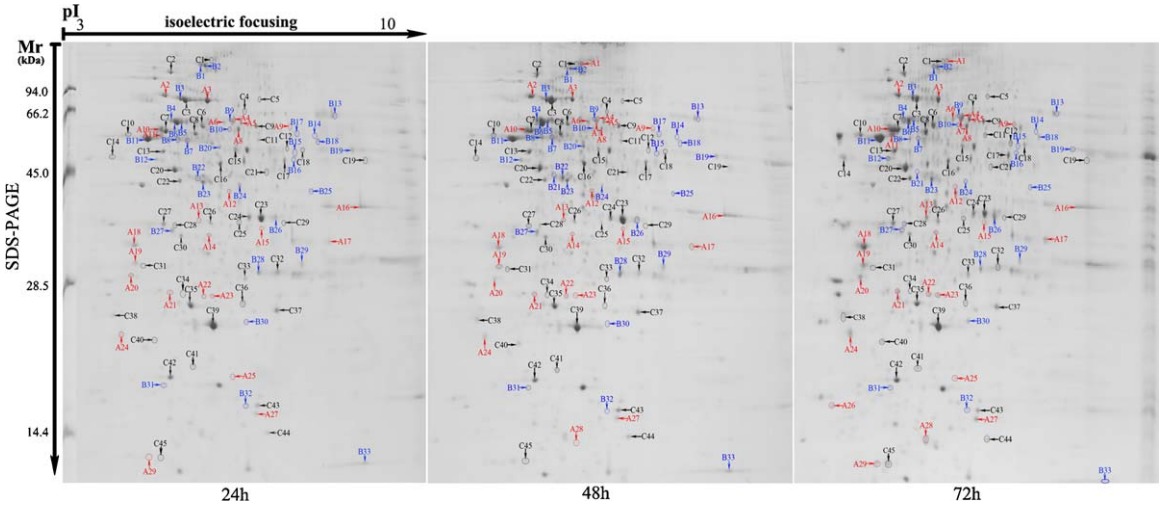

Fig. 1. 2-DE profile of drone eggs (*A. m. ligustica*) at 24, 48, and 72 h, respectively. 280 μg of each sample was subjected to 2-DE and stained by CBB G-250. Quantitative differences are indicated by color coded letter/number (An or Bn), red "An" and blue "Bn" represent up-regulation and down-regulation, respectively, while black "Cn" indicate no significant differences. (For interpretation of the references to color in this figure legend, the reader is referred to the web version of the article.)

Table 2
Identification of differentially expressed proteins during the embryogenesis of the honeybee drone (*Apis mellifera* L.).

Spot number	Experimental pI/Mr (kDa)	Theoretical pI/Mr (kDa)	Sequence coverage	Matched/ searched	Score	Protein name	Accession number	Mean ± SD			Identification method
								24 h	48 h	72 h	
Carbohydrate and energy metabolism											
B19	8.12/51.95	9.00/59.76	31%	18/23	181	ATP synthase subunit α (blw)	gi|48100966	18994.4± 1592b	27567 ± 1580a	21307.8 ± 1750b	MALDI-TOF
A15	6.83/32.46	6.26/36.47	41%	14/89	95	Aldehyde reductase (EC.1.1.1.21)	gi|66525576	4250.2 ± 340c	6017.6 ± 791b	7689.9 ± 549a	MALDI-TOF Q-TOF
B26	5.29/10.12	6.26/36.06	39%	44/655	631			18514.5 ± 968b	33350.1 ± 1456a	17967.9 ± 1356b	
B29	7.33/26.99	9.36/35.40	35%	13/30	118	Phosphoglyceromutase (pglym78, EC.5.4.2.1)	gi|66550890	16162.9 ± 500a	17244 ± 642a	10375.9 ± 480b	MALDI-TOF
B13	7.85/64.70	7.62/67.78	22%	12/25	112	Transketolase (EC.2.2.1.1)	gi|110751363	31078.8 ± 1340a	29664.2 ± 1189a	18201.7 ± 890b	MALDI-TOF
B25	7.52/40.79	7.57/39.98	34%	7/15	91	Fructose-bisphosphate aldolase (ald, EC.4.1.2.13)	gi|110748949	12442.1 ± 495a	7392.3 ± 250b	6798.9 ± 561b	MALDI-TOF
B20	6.03/54.57	6.69/55.94	32%	15/41	110	Aldehyde dehydrogenase (EC.1.2.1.3)	gi|66530423	11725.3 ± 490a	13082.3 ± 720a	0 ± 0	MALDI-TOF
A7	6.36/62.84	6.03/59.90	31%	16/80	709	ATP phosphohydrolase (EC.3.6.1.3)	gi|66540596	0 ± 0	15952.1 ± 920a	18231.5 ± 680a	Q-TOF
B10	6.29/60.58	6.22/57.87	16%	6/77	172		gi|66533395	4814.8 ± 240b	10718.7 ± 840a	6130.9 ± 510b	Q-TOF
B17	7.21/59.96	7.10/57.86	46%	25/171	1125		gi|66558942	642.4 ± 42	0 ± 0	0 ± 0	Q-TOF
A8	6.48/60.46	6.22/58.32	61%	45/250	1720		gi|66533395	26143 ± 1452b	27071.1 ± 1689b	40223.7 ± 2356a	Q-TOF
B33	8.43/11.42	8.01/11.40	81%	11/114	496		gi|66547447	6941.1 ± 502b	27239.1 ± 1056a	11572.9 ± 1250b	Q-TOF
B16	7.32/49.24	6.79/52.88	37%	20/128	743	6-Phosphogluconate dehydrogenase (pgd, EC.1.1.1.44)	gi|66547531	8012.6 ± 420a	9303.1 ± 801a	4101.8 ± 401b	Q-TOF
B14	7.61/57.41	7.68/58.22	9%	4/223	118	glucose-1-phosphate uridylyltransferase (ugp, EC.2.7.7.9)	gi|66536233	5609.9 ± 432a	4253.7 ± 512b	2509.9 ± 126c	Q-TOF
B23	5.66/44.30	5.66/40.33	43%	18/61	114	Arginine kinase (argk, EC.2.7.3.3)	gi|58585146	27203.1 ± 1125b	42868.6 ± 989a	30899.2 ± 1021b	MALDI-TOF
B22	5.55/45.21		37%	18/646	353			62224.3 ± 2980a	43734.7 ± 2351b	0 ± 0	Q-TOF
B12	5.02/49.35	5.34/53.94	20%	13/127	542	Ubiquinol-cytochrome-c reductase (ox, EC.1.10.2.2)	gi|66500205	9901.7 ± 504b	17814.601 ± 980a	10638.4 ± 750b	Q-TOF
A28	5.68/16.27	8.67/14.39	22%	2/394	59	Cytochrome-c oxidase (cox5b, EC.1.9.3.1)	gi|66534766	0 ± 0	2421.8 ± 240b	12192.7 ± 680a	Q-TOF
A16	8.19/27.62	7.60/31.91	33%	8/12	94	Glyceraldehyde 3 phosphate dehydrogenase (EC.1.2.1.12)	gi|66517066	21870.6 ± 1205c	62224.3 ± 2560a	43734.7 ± 1980b	MALDI-TOF
Amino acid metabolism											
A14	5.72/32.37	5.87/34.71	47%	15/35	102	26S proteasome non-ATPase regulatory subunit 14	gi|66552230	2408.1 ± 180b	7834.1 ± 220a	8161 ± 370a	MALDI-TOF
A20	4.70/26.50	4.83/57.00	26%	16/120	427	Proteasome subunit α type 5 (prosma5)	gi|66541426	9259.8 ± 610b	10715.2 ± 840b	16851.9 ± 690a	Q-TOF
B30	6.34/22.78	6.44/23.79	42%	11/45	82	Proteasome subunit β type	gi|66519157	6199.3 ± 684b	17955.9 ± 1570a	9989.8 ± 980b	MALDI-TOF
A22	5.48/25.59	5.67/26.07	30%	26/	325	Proteasome subunit β type 1 (EC.3.4.25.1)	gi|66512107	4243.6 ± 256b	10225.8 ± 747a	10734.4 ± 691a	Q-TOF
A23	5.92/25.54	6.90/28.76	26%	14/469	229	Proteasome subunit β type 4 precursor (EC.3.4.25.1)	gi|48100320	5708 ± 680c	11230.9 ± 682b	12656.4 ± 708a	Q-TOF
Nucleotide and fatty acid metabolism											
B24	6.41/42.09	6.16/47.06	24%	9/19	94	Acyl-CoA dehydrogenase (ACAD1) (EC.1.3.99.3)	gi|110763684	14066.5 ± 1020a	12828.8 ± 840a	8385.4 ± 651b	MALDI-TOF
B27	5.07/32.27	5.15/34.12	31%	28/693	491	4-Nitrophenylphosphatase (EC.3.1.3.41)	gi|48141571	18314.4 ± 950b	21967.9 ± 1250a	8894 ± 681c	Q-TOF
Cytoskeleton											
B11	4.97/56.68	4.75/50.61	33%	19/24	204	Tubulin β-1 chain (βtub56d)	gi|48095525	86898.3 ± 3245b	110360.3 ± 5642a	72855.7 ± 3218b	MALDI-TOF
A10	5.06/59.59	5.01/50.63	42%	14/70	97	Tubulin α-1 chain (αtub84d)	gi|66521545 gi|66535209	36437.6 ± 2500c	58090 ± 3651b	75899.3 ± 2489a	MALDI-TOF
B3	5.31/73.10		39%	13/34	119			44284 ± 921a	36709 ± 1256b	28218.6 ± 726c	MALDI-TOF
B8	5.17/57.33	4.77/42.63	23%	7/9	89	β Tub56D	gi|24655746	16101.4 ± 680b	28964.3 ± 1520a	12379.8 ± 950b	MALDI-TOF
A26	3.67/18.82	5.29/41.85	15%	3/205	93	Actin	gi|1703112	0 ± 0	0 ± 0	9493.7 ± 580	Q-TOF
Development											
A18	4.80/29.10	4.78/29.09	42%	9/21	116	14-3-3 protein epsilon	gi|48096523	32240 ± 2000b	38299.4 ± 1500b	69804.8 ± 2578a	MALDI-TOF

Table 2 (*Continued*)

Spot number	Experimental pI/Mr (kDa)	Theoretical pI/Mr (kDa)	Sequence coverage	Matched/ searched	Score	Protein name	Accession number	Mean ± SD			Identification method
								24 h	48 h	72 h	
A27	6.56/17.68	6.75/17.69	59%	7/11	110	Nucleoside diphosphate kinase (awd, EC.2.7.4.6)	gi|66520497	10443.2 ± 510b	20887.8 ± 894a	21918.4 ± 1021a	MALDI-TOF
B28	6.69/26.41	6.54/30.00	57%	10/21	136	Protein lethal (2) 37Cc [l(2)37cc]	gi|48097857	25588.6 ± 1024b	46523.1 ± 1129a	28796.8 ± 1354b	MALDI-TOF
B31	4.97/19.22	5.33/10.45	22%	2/129	94	Ubiquitin-like protein smt3 (smt3)	gi|66549336	12248.6 ± 650a	13865.8 ± 721a	5264.6 ± 350b	Q-TOF
A19	4.76/27.38	4.79/28.06	38%	2/163	465	14-3-3-like protein	gi|48097086	12876.9 ± 620b	11979.6 ± 570b	26225.3 ± 1203a	Q-TOF
A1	6.26/152.08	6.29/200.92	7%	10/66	299	Vitellogenin	gi|58585104	0 ± 0	2760 ± 140b	3669.2 ± 210a	Q-TOF
A24	4.50/21.76	4.57/19.83	48%	12/198	479	Translationally-controlled tumor protein homolog (TCTP)	gi|66515987	8091.5 ± 520c	14521.2 ± 689b	27138.3 ± 1450a	Q-TOF
A17	7.70/29.58	7.62/32.26	39%	16/96	82	Guanine nucleotide-binding protein subunit β (gbeta13f)	gi|48104663	13647.7 ± 1371b	13094.2 ± 1120b	24994.6 ± 1840a	MALDI-TOF
B21	5.35/45.56	5.47/48.11	22%	15/634	298	COP9 signalosome complex subunit 4 (CSN4)	gi|66521456	0 ± 0	16014.4 ± 1323a	2318.6 ± 456b	Q-TOF
B18	7.45/52.62	6.52/42.14	22%	7/11	97	Imaginal disc growth factor 4 (idgf4)	gi|110773851	17600.2 ± 970a	11411 ± 880b	7531.9 ± 420c	MALDI-TOF
Antioxidant system											
A21	5.03/25.70	5.40/17.69	41%	6/20	82	Glutathione S transferase S1 (gsts1, EC.2.5.1.18)	gi|66534655	5566 ± 540b	9148.1 ± 470a	4573.7 ± 320b	MALDI-TOF
B32	6.42/18.07	6.22/15.80	15%	8/154	233	Superoxide dismutase (sod, EC.1.15.1.1)	gi|66513527	5394.9 ± 410b	9418.4 ± 680a	5596.4 ± 350b	Q-TOF
A25	6.08/19.41	6.12/20.28	74%	11/45	126	dj-1β	gi|66531474	4926 ± 350a	0 ± 0	5851.6 ± 405a	MALDI-TOF
Transcription/translation											
A12	6.18/39.78	6.13/39.50	44%	11/28	111	Translation initiation factor 2B (eif2b)	gi|48096956	2595.4 ± 180c	15215 ± 890a	12149.6 ± 780b	MALDI-TOF
A29	4.88/14.77	5.16/14.80	23%	3/152	109	Nuclear transport factor-2 (Ntf-2)	gi|48104167	3978 ± 325b	4341.6 ± 652b	8231.9 ± 521a	Q-TOF
A13	5.48/35.04	5.75/34.39	34%	31/627	461	60S acidic ribosomal protein P0 (rplp0)	gi|66559310	6398.4 ± 368c	12038.5 ± 689b	20510.7 ± 756a	Q-TOF
B15	7.34/52.17	7.18/44.26	24%	9/101	426	Methionyl aminopeptidase (PA2G4, EC.3.4.11.18)	gi|66507356	5566 ± 540b	9148.1 ± 470a	4573.7 ± 320b	Q-TOF
Protein folding											
A2	5.10/73.71	5.29/72.88	19%	14/18	157	Heat shock protein cognate 3 (hsc70-3)	gi|229892214	16939.601 ± 3200b	31911.7 ± 2402a	15057.2 ± 1520a	MALDI-TOF
A4	6.42/64.21	6.03/60.42	34%	15/57	92	T-complex protein 1 eta (T-complex	gi|66540596	18300.6 ± 652a	8188.7 ± 521b	24040.9 ± 950a	MALDI-TOF
A6	6.17/63.14		31%	17/41	116	protein, EC.3.6.1.3)		5964.8 ± 260b	15623.4 ± 745a	14095.6 ± 956a	MALDI-TOF
B2	5.90/94.76	5.83/91.96	35%	23/59	149	hsc70Cb	gi|66505007	18556.4 ± 921b	35703.6 ± 1250a	16227.9 ± 810b	MALDI-TOF
B1	5.86/95.28		25%	14/24	132			5975.8 ± 291b	11548.8 ± 520a	6618.6 ± 320b	MALDI-TOF
B9	6.33/64.42	6.58/43.93	26%	12/119	571	T-complex protein 1 zeta (tcp-20, EC.3.6.1.3)	gi|66513205	15161.2 ± 980a	10694.5 ± 890b	7812.8 ± 456b	Q-TOF
A5	6.55/62.98	6.58/44.21	46%	25/329	1027			13735.6 ± 1250b	19794.6 ± 1156b	32943.4 ± 1426a	Q-TOF
B7	5.38/55.82	5.47/51.50	4%	2/59	43	FK506-binding protein 59 (EC.5.2.1.8)	gi|66499186	14362.9 ± 1204a	19447.3 ± 950a	7567 ± 350b	Q-TOF
A9	7.29/58.93	7.10/57.34	19%	9/321	180	T-complex protein 1 delta subunit (tcp-1-delta, EC.3.6.1.3)	gi|66558942	3553.5 ± 256b	5689.9 ± 461a	6561.4 ± 423a	Q-TOF
B4	5.14/63.48	5.64/60.55	26%	14/291	506	60 kDa heat shock protein	gi|66547450	35832.701 ± 2400a	37469.1 ± 1980a	23855.9 ± 1060b	Q-TOF
B5	5.52/71.12		65%	73/743	1131			29974.4 ± 1480a	24150.6 ± 1598b	13042.4 ± 568c	Q-TOF
B6	5.18/62.53		26%	13/25	131			45532.9 ± 4237b	93021.9 ± 7428a	76120.8 ± 3842b	MALDI-TOF
A11	5.05/56.93	5.27/30.20	26%	8/138	345	Protein disulfide-isomerase precursor (pdi)	gi|66531851	16916 ± 1254b	0 ± 0	29943.6 ± 1240a	Q-TOF
A3	5.89/72.68	5.47/75.65	69%	109/770	1477	Heat shock protein cognate 5 (hsc70-5)	gi|66501507	46067 ± 2980a	36053.6 ± 2681b	61571.1 ± 2356a	Q-TOF

All the identified proteins were hit against *A. mellifera* except B8 that hit against Drosophila. Spot number corresponds to the number of protein spots in Fig. 2A. Theoretical molecular weight (Mr) and isoelectric point (p*I*) of the identified proteins were retrieved from the protein database of NCBInr. Experimental Mr and p*I* were calculated with PDQuest Software and internal standard molecular mass markers. Sequence coverage is the ratio of the number of amino acids in every peptide that matches with the mass spectrum divided by the total number of amino acids in the protein sequence. Matched peptide is the number of paring an experimental fragmentation spectrum to a theoretical segment of protein and searched is the total searched peptide. Mascot score is search against the database NCBInr. Protein name is given when proteins were identified by MALDI-TOF/MS and LC-Chip/ESI-QTOF-MS. Accession number is the unique number given to mark the entry of a protein in the database NCBInr.

Table 3
Identified proteins without differential expression during the embryogenesis of honeybee drone (*Apis mellifera* L.).

Spot number	Experimental pI/Mr(kDa)	Theoretical pI/Mr(kDa)	Sequence coverage	Matched/ searched	Score	Protein name	Accession number	Identified method
Carbohydrate and energy metabolism								
C2	5.17/89.54	5.18/89.48	27%	19/47	106	Transitional endoplasmic reticulum ATPase	gi|66534286	MALDI-TOF
C13	5.06/52.29	5.25/55.10	60%	24/37	287	ATP synthase subunit β (atpsyn-β, EC.3.6.3.14)	gi|110762902	MALDI-TOF
C23	6.84/34.67	6.26/36.47	26%	8/24	84	Aldehyde reductase (EC.1.1.1.21)	gi|66525576	MALDI-TOF
C24	6.58/35.03	6.26/36.06	39%	65/714	824			Q-TOF
C19	8.22/49.05	8.15/45.14	32%	13/23	119	Phosphoglycerate kinase (EC.2.7.2.3)	gi|110763826	MALDI-TOF
C28	5.15/33.63	6.31/83.86	15%	11/308	231	Inorganic pyrophosphatase (nurf-38, EC.3.6.1.1)	gi|66507623	Q-TOF
C29	7.06/33.38	6.25/36.19	35%	13/123	493	Malate dehydrogenase (EC.1.1.1.37)	gi|66506786	Q-TOF
C40	4.91/21.29	5.00/20.32	35%	7/18	82	ATP synthase D chain (atpsyn-d)	gi|48098315	MALDI-TOF
C25	6.54/28.73	6.15/29.63	45%	37/375	663	Dehydrogenases	gi|110759030	Q-TOF
C15	6.17/50.72	5.51/40.12	23%	26/630	335	2-Phosphoglycerate dehydratase (EC.4.2.1.11)	gi|110761968	Q-TOF
Amino acid metabolism								
C33	6.43/27.09	7.03/30.29	20%	9/721	191	Proteasome 2 (EC.3.4.25.1)	gi|66519842	Q-TOF
C26	5.77/34.29	5.78/30.91	34%	22/625	350	Proteasome subunit α type 1 (EC.3.4.25.1)	gi|66530404	Q-TOF
Fatty acid metabolism								
C21	6.95/45.49	8.51/46.84	39%	14/59	87	Acyl-CoA dehydrogenase (EC.1.3.99.3)	gi|66499429	MALDI-TOF
Cytoskeleton								
C4	6.65/66.83	6.32/67.43	28%	14/35	126	Putative actin-interacting protein 1	gi|66538420	MALDI-TOF
C7	5.09/59.91	5.01/50.63	46%	19/84	121	Tubulin alpha-1 chain	gi|66521545	MALDI-TOF
C30	5.14/31.28	5.37/32.84	33%	13/733	311	F-actin capping protein subunit α	gi|66508517	Q-TOF
C41	5.19/19.95	6.17/16.82	64%	49/424	434	Cofilin/actin-depolymerizing factor homolog (tsr)	gi|110751158	Q-TOF
Development								
C37	7.03/24.86	6.96/24.86	48%	13/100	90	GTP-binding nuclear protein Ran (ran)	gi|48097366	MALDI-TOF
C31	4.86/27.40	4.79/28.17	48%	2/148	117	14-3-3-like protein	gi|48097086	Q-TOF
C32	7.02/26.45	6.97/26.08	49%	11/52	91	Calcyclin binding protein	gi|66564402	MALDI-TOF
C22	5.16/43.66	5.31/38.07	12%	4/67	144	Nuclear migration protein nudC	gi|66518451	Q-TOF
C44	6.83/16.93	6.81/16.90	11%	2/98	88	Suppressor of GMR-sina 3-3 (eff)	gi|24646906	Q-TOF
C36	6.31/25.17	6.10/25.34	51%	15/44	102	Ferritin 2 light chain homologue (Fer2LCH, EC.1.-.-.-)	gi|66524161	MALDI-TOF
C10	4.83/55.91	4.72/48.15	14%	17/610	196	Chromatin assembly factor 1 subunit (acf1)	gi|66534191	Q-TOF
Antioxidant system								
C39	5.70/21.95	5.65/21.95	49%	7/13	110	Thioredoxin peroxidase (EC.1.11.1.15)	gi|66548188	MALDI-TOF
C35	5.19/25.19	5.40/17.69	37%	11/175	463	Glutathione S transferase S1 (EC.2.5.1.18)	gi|66534655	Q-TOF
C12	7.21/52.91	6.90/53.22	46%	21/274	539	Thioredoxin reductase (trxr-1, EC.1.8.1.9)	gi|33089108	Q-TOF
C18	7.44/52.66	6.22/53.22	22%	12/169	502			
C43	6.67/18.03	6.21/15.80	54%	10/152	482	Superoxide dismutase (EC.1.15.1.1)	gi|66513527	Q-TOF
C45	5.10/11.80	4.82/12.18	13%	2/94	135	Thioredoxin-2 (trx-2, EC.1.8.1.8)	gi|48104680	Q-TOF
C34	4.96/19.95	5.30/24.91	34%	18/775	255	Peroxiredoxin-6 (EC.1.11.1.15)	gi|66521517	Q-TOF
Transcription/translation								
C16	6.00/49.30	6.02/49.25	46%	22/142	101	Translation elongation factor 1-γ (efly)	gi|110761214	MALDI-TOF
C11	6.88/55.99	6.32/50.16	32%	10/22	94	RuvB-like protein 1 (EC.3.6.1.-)	gi|48106137	MALDI-TOF
C42	5.02/19.51	5.19/17.58	48%	10/194	404	Eukaryotic translation initiation factor 5A (eif-5a)	gi|110767655	Q-TOF
C17	7.32/48.70	8.16/52.39	43%	27/205	957	Elongation factor Tu isoform 2 (eftum)	gi|66518848	Q-TOF
Protein folding								
C20	5.14/47.12	5.29/72.88	31%	20/83	86	Heat shock protein cognate 3	gi|229892214	MALDI-TOF
C3	5.40/72.10	5.43/71.39	42%	30/51	238	Heat shock protein cognate 4	gi|229892210	MALDI-TOF
C6	5.64/64.22	5.69/60.60	35%	16/65	98	T-complex protein 1 subunit α (cct5, EC.3.6.1.3)	gi|66560172	MALDI-TOF
C8	5.58/59.35	5.57/56.23	41%	20/28	233	Protein disulfide-isomerase (EC.5.3.4.1)	gi|66546657	MALDI-TOF
C9	6.86/60.91	6.24/55.79	31%	15/49	86	Hsp70/Hsp90 organizing protein (hop)	gi|110756123	MALDI-TOF
C5	6.95/72.05	8.49/79.93	20%	10/22	86	TNF receptor-associated protein 1 (EC.4.1.2.13)	gi|66511337	MALDI-TOF
C1	6.19/101.25	5.83/91.96	22%	14/24	132	Hsc70Cb	gi|66505007	MALDI-TOF
C14	4.54/46.82	4.49/37.75	20%	5/122	209	Supercoiling factor (EC.5.99.1.-)	gi|66509518	Q-TOF
Unknown function								
C38	4.36/24.93	4.55/17.22	17%	2/130	96	Putative uncharacterized protein (EC.5.2.1.8)	gi|66510528	Q-TOF
C27	5.01/33.49	5.38/40.91	40%	63/722	700	Yellow-g	gi|48137874	Q-TOF

All the identified proteins were hit against *A. mellifera* except C44 that hit against Drosophila. Spot number corresponds to the number of protein spots in Fig. 2B. Theoretical molecular weight (Mr) and isoelectric point (p*I*) of the identified proteins were retrieved from the protein database of NCBInr. Experimental Mr and p*I* were calculated with PDQuest Software and internal standard molecular mass markers. Sequence coverage is the ratio of the number of amino acids in every peptide that matches with the mass spectrum divided by the total number of amino acids in the protein sequence. Matched peptide is the number of paring an experimental fragmentation spectrum to a theoretical segment of protein and searched is the total searched peptide. Mascot score is search against the database NCBInr. Protein name is given when proteins were identified by MALDI-TOF/MS and LC-Chip/ESI-QTOF-MS. Accession number is the unique number given to mark the entry of a protein in the database NCBInr.

protein folding. In addition, there were three development related proteins (spots B21, B28 and B31), two cytoskeletal proteins (spots B8 and B11), two translation regulation proteins (spots A12 and B15), two nucleic acid metabolism-related proteins (spot B27 and B30) and one antioxidant protein (spot B32) that were all up-regulated at the 48 h embryonic age (Fig. 3).

At the 72 h embryonic age 25 proteins were highly expressed. As compared with the 24 and 48 h embryonic ages, most of the proteins (spots A27, A1, A17, A18, A19 and A24) were involved in development. Proteins involved in folding (spots A9, A5, A4, A11 and A3) remained the second largest family as was the case for the 24 and 48 h embryonic ages.

Interestingly, there was a fewer number of upregulated proteins (spots A7, A8, A28 and A15) related to carbohydrate metabolism and energy production at 72 h than those at 24 and 48 h. Translation (spots A29 and A13), cytoskeleton (spots A26 and A10) and antioxidation-related proteins (spots A21 and A25) were also highly expressed at 72 h (Fig. 3). Furthermore, four amino acid metabolism-related proteins (spots A14, A22, A23 and A20) were uniquely expressed at this age.

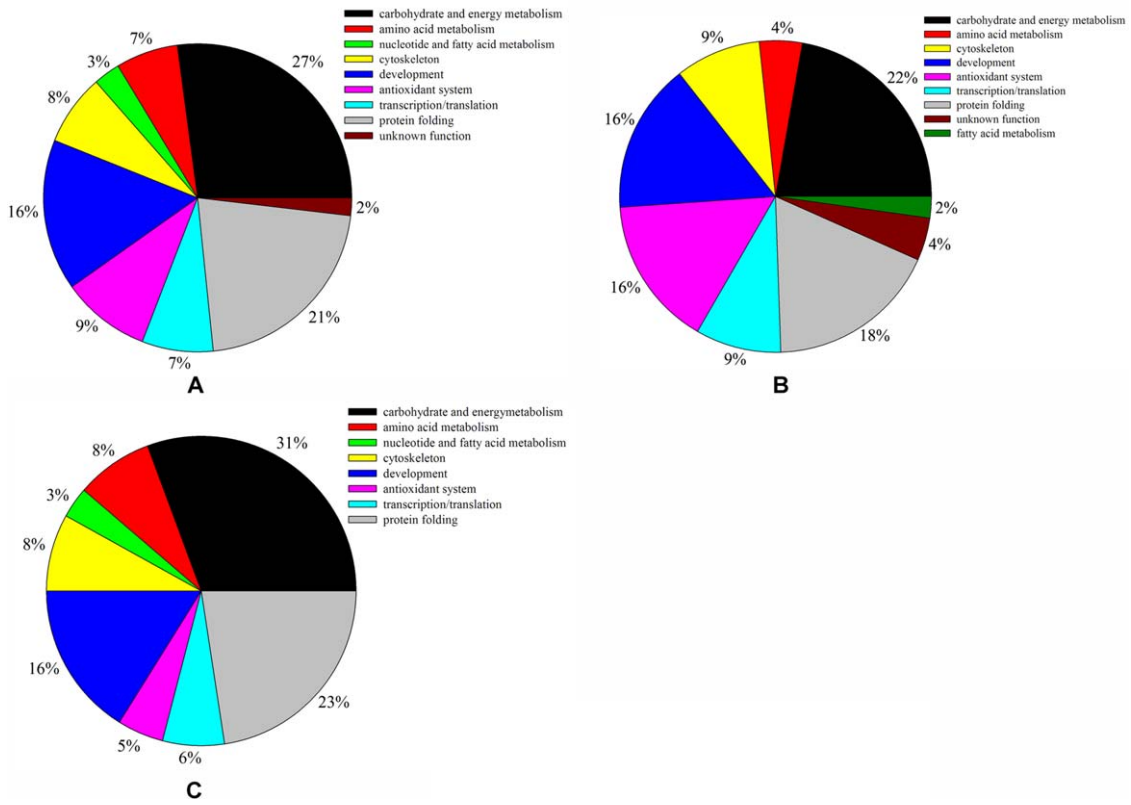

Fig. 2. Pie charts represent the proportion of functional classifications of the identified proteins. (A) Represents the proportion of functional classifications across all the time points, (B) represents the proportion of stable expressed proteins, while (C) represents the proportion of differentially regulated proteins.

3.3. Protein networks

Pathway Studio (Ariadne Genomics) was used to assist interpretation of the experimental results based on the context of pathways, protein regulation networks, and protein interaction maps in the *Drosophila* molecular networks database. A total of 49 proteins were identified by interactions between the imported proteins and all proteins stored in the database and were classified into six functional groups (Fig. 4). Accordingly, proteins involved in carbohydrate metabolism and energy production were the most abundant in the networks (28.6% or 14 proteins): ATP phosphohydrolase (spots A8), cox5b (spot A28), aldehyde reductase (spot A15), ox (spot B12), ugp (spot B14), pgd (spot B16), blw (spot B19), argk (spot B22), pglym78 (spot B29), transketolase (spot B13), ald (spot B25), atpsyn-β (spot C13), nurf-38 (spot C28), and atpsyn-d (spot C40). The second abundant (22.5% or 11 proteins) group was a family of proteins mainly involved in the regulation of development. They were gbeta13f (spot A17), TCTP (spot A24), awd (spot A27), idgf4 (spot B18), CSN4 (spot B21), l(2)37cc (spot B28), smt3 (spot B31), acf1 (spot C10), Fer2LCH (spot C36), ran (spot C37), and eff (spot C44). Proteins with folding functions were the third most abundant group (16.3% or 8 proteins) in the link. These proteins were hsc70-3 (spot A2), hsc70-5 (spot A3), tcp-20 (spot A5), tcp-1-delta (spot A9), pdi (spot A11), T-complex protein (spot A4), cct5 (spot C6) and hop (spot C9). There were seven proteins designated as the fourth category in the network and were mainly related to transcription/translation. They were eif2b (spot A12), rplp0 (spot A13), Ntf-2 (spot A29), PA2G4 (spot B15), efly (spot C16), eftum (spot C17) and eif-5a (spot C42). Additionally, three cytoskeleton proteins, αtub84d (spot A10), βtub56d (spot B11) and tsr (spot C41), and four antioxidant proteins, gsts1 (spot A21), sod (spot B32), trxr-1 (spot C18) and trx-2 (spot C45), and amino acid metabolism protein prosma5 (spot A20) and a fatty acid metabolism ACAD1 (spot B24) were observed in the network.

To confirm differentially expressed proteins at the transcriptional level, 13 genes from four major functional groups (carbohydrate metabolism and energy production, protein folding, development and antioxidation) were selected for qRT-PCR analysis. The trend of mRNA expression of eight genes (tcp-1-delta (spot A9), αtub84d (spot A10), 26S proteasome non-ATPase regulatory subunit (spot A14), gsts1 (spot A21), TCTP (spot A24), awd (spot A27), smt3 (spot B31) and ATP phosphohydrolase (spot B33)) appeared the same as protein expression (Fig. 5). However, a diverse pattern between mRNA and protein expression was seen in another five genes: T-complex protein (spot A4), pdi (spot A11), cox5b (spot A28), Ntf-2 (spot A29) and βtub56d (spot B11) (Fig. 5).

4. Discussion

We report in this study, the proteomic analysis of honeybee male embryogenesis, based on 2-DE, complimentary MS and bioinformatic tools. More than 100 expressed proteins during drone embryogenesis were characterized. Twenty-four hour old embryos were at the initial stage of embryogenesis and exhibited less up-regulated proteins expression. By contrast, the middle age (48-h old) was the most active stage for embryos to express proteins, especially carbohydrate and energy production-related proteins. The older embryos (72-h old), however, expressed more development-related proteins. These findings suggest that organogenesis mainly occurred at the middle to late stage of embryogenesis. The result is similar to a previous study that showed the 36–44 h embryonic period is the time for worker embryo to initiate differentiation, whereas 16–18 h embryos have slow proliferation and no sign of cell differentiation (Bergem et al., 2006). The identified protein spots whose abundance as stable over time suggests their conservative roles as housekeeping proteins to support drone embryogenesis.

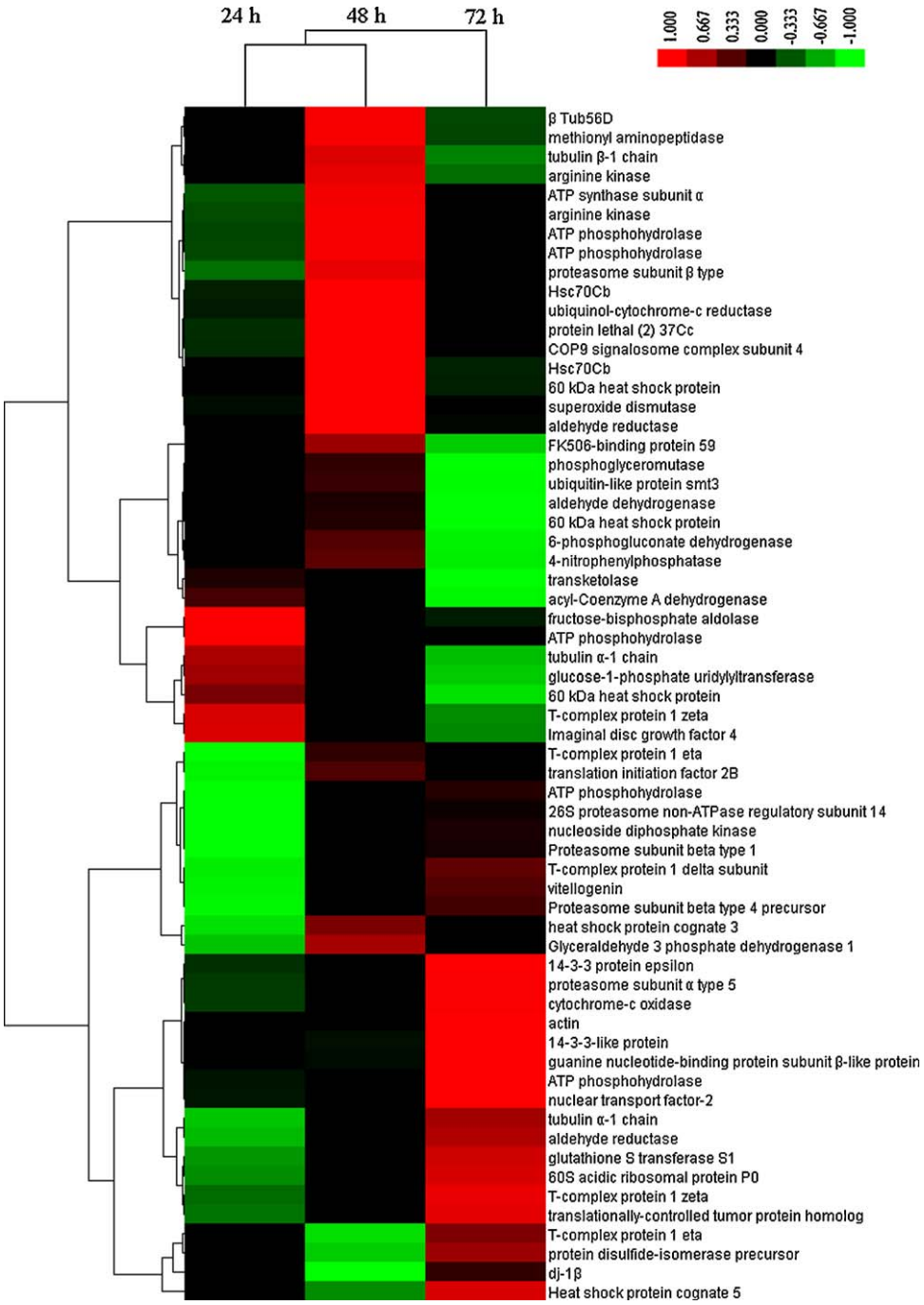

Fig. 3. Hierarchical clustering analysis of 62 differentially expressed proteins at 24, 48 and 72-h old drone embryo. The 3 columns represent the drone bee embryos at 24, 48 and 72 h. The rows represent the individual protein. The proteins cluster is on the left, and the development time is on the top. The up- or down-regulated proteins are indicated in red and blue, respectively. The intensity of the colors increases with increasing expression differences as noted on the key bar on the top right side. Protein name is indicated on the right. (For interpretation of the references to color in this figure legend, the reader is referred to the web version of the article.)

Protein grouping analysis shows that carbohydrate metabolism and energy production, folding and development-related proteins represented 65% of the total proteins identified, indicating the significance of these proteins in drone embryogenesis. The honeybee displays four distinct stages in its life cycle, each with radically different body plans: egg, larva, pupa and adult. Large amounts of carbohydrate metabolism and energy production are needed by the developing embryos to undergo a series of organogenesis. Our findings indicates that 48 h is a milestone of drone embryo differentiation. This is in line with previous studies that embryos complete neural tube closure and head involution at 48 h (Collins et al., 2004; Winston, 1987). The embryonic age of 48 h is a particular developmental point at which the developing embryo demands high amounts of these protein species. The carbohydrate metabolism and energy production required by the developing embryos at 48 h may be the result of the initiation of metamorphosis and programmed cell division by the developing tissues which results in the transformation of active embryo to larva (Li et al., 2007, 2009; Winston, 1987).

Proteins with folding function such as Hsps, have been documented as a defensive response protein to stress factors in salivary glands (Silva-Zacarin et al., 2006), larvae (Gregorc, 1998; Gregorc and Bowen, 1999), bacteria and heat treated adult honeybees (Severson et al., 1990). It has also been reported as a

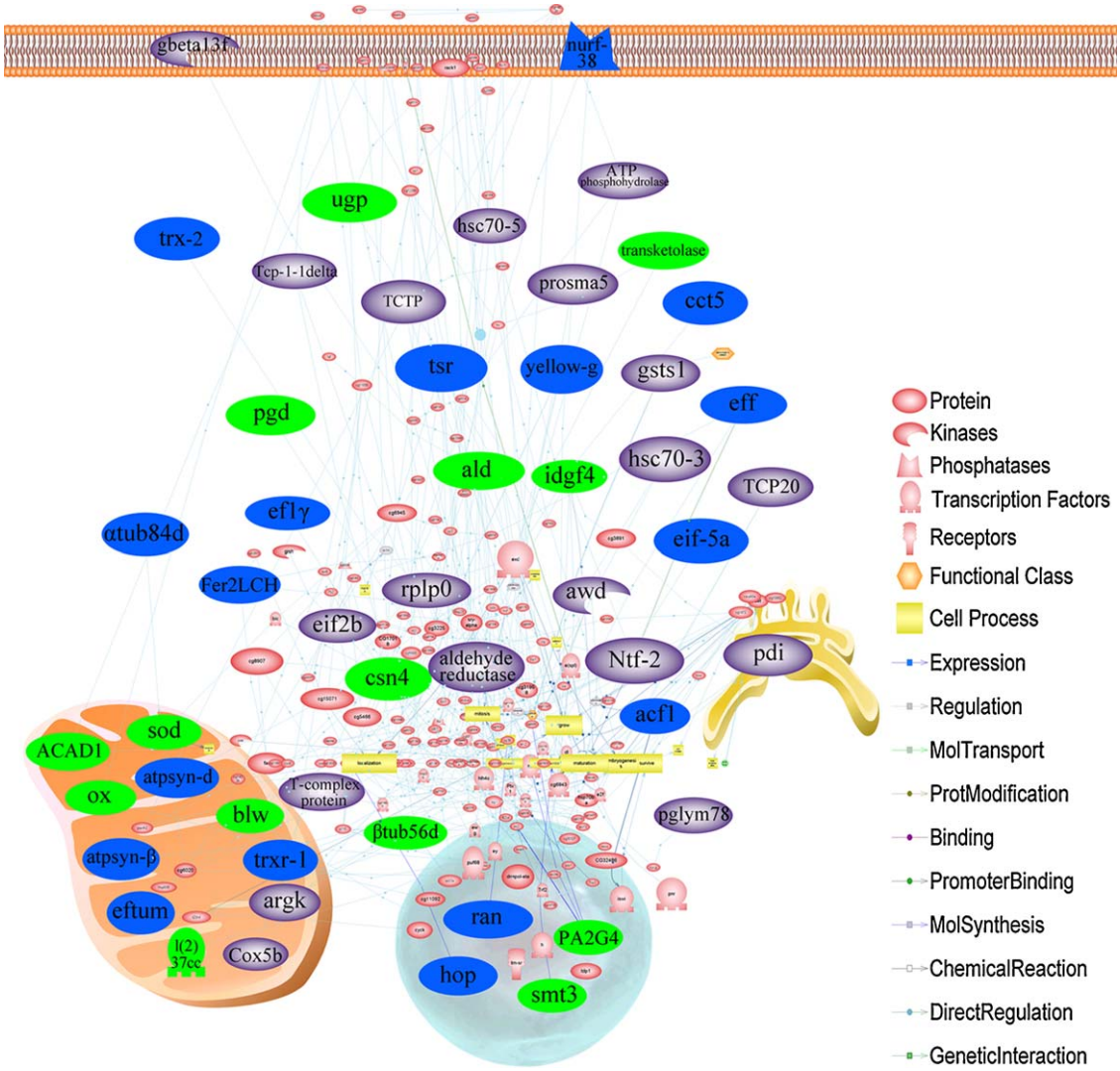

Fig. 4. Network analysis of all the pathway and interactions connected to all the identified proteins. Those highlighted in purple and green represent the up-or-down-regulated key node proteins, respectively and those blue indicates protein nodes with no significant change. Meanwhile, the yellow triangles represent the deferentially regulated proteins. Protein entities which belong to different functional groups were automatically represented to different shapes according to the default settings of the software, "sickle" "red ellipse" for proteins, "sickle" for kinases, "rhomb" for ligands, "stick" for receptors, "O-vertex" for transcription factors, "2 triangles" for phosphates, "grey ellipse" for cell objects, "orange hexagon" and "yellow rectangle" for cell process. (For interpretation of the references to color in this figure legend, the reader is referred to the web version of the article.)

molecular chaperone under normal physiological conditions (De Maio, 1999; Hirsch et al., 2006) in the honeybee worker larvae (Li et al., 2007), head and brain (Garcia et al., 2009), hemolymph (Chan et al., 2006), venom gland (Peiren et al., 2008) and hypopharyngeal gland (Feng et al., 2009). It should be noted that the outer covering of the nervous system and the organs of the digestive system are formed during embryogenesis. There is a constant up-regulation of these proteins at 48 and 72 h. This indicates a possible role in aiding organogenesis by folding newly synthesized proteins, binding other non-native proteins and assisting them in reaching the correctly folded and functional conformation (Borges and Ramos, 2005).

The expression of proteins involved in development was significantly increased at the embryonic age of 72 h. Smt3 is known to be involved in the synthesis of ecdysteroid (Talamillo et al., 2008). In *Drosophila*, TCTP is known as a positive regulator of cell size, eye growth, and growth of the first posterior cell and the wing (Hsu et al., 2007). Awd is involved in the development of the embryonic dorsal trunk, tracheal system, dorsal group branch (Molnar et al., 2006; Woolworth et al., 2009; Xu et al., 1996). CSN4 is regulator of multiple pleiotropic pathways in compound eye photoreceptor cell differentiation and cephalopharyngeal skeleton (Oron, 2002). Idgf is cofactor of insulin or insulin like peptide (Gregorc, 1998). Gbeta13f is involved in asymmetric neuroblast division (Katanaev, 2006) and (2)137cc is associated with the development of larvae and hypopharyngeal gland (Feng et al., 2009; Li et al., 2007, 2009). Vitellogenin has versatile regulatory functions in honeybees and has been well documented for its role in the regulation of honeybee development. Primarily, foraging and swarming behavior (Hrassnigg and Crailsheim, 2005; Zeng et al., 2005). Vitellogenin also acts as an antioxidant to prolong the queen bee and forager lifespan, and affects multiple physiological processes (Amdam et al., 2004; Nelson et al., 2007; Seehuus et al., 2006). The increased expression of vitellogenin in the drone embryos probably stimulates embryogenesis. To emphasize, our present study showed that high expression of proteins involved in developmental regulation occur in the late phase of the drone embryo. This suggests the importance of development–related proteins in organogenesis for formation and development of the basic organs

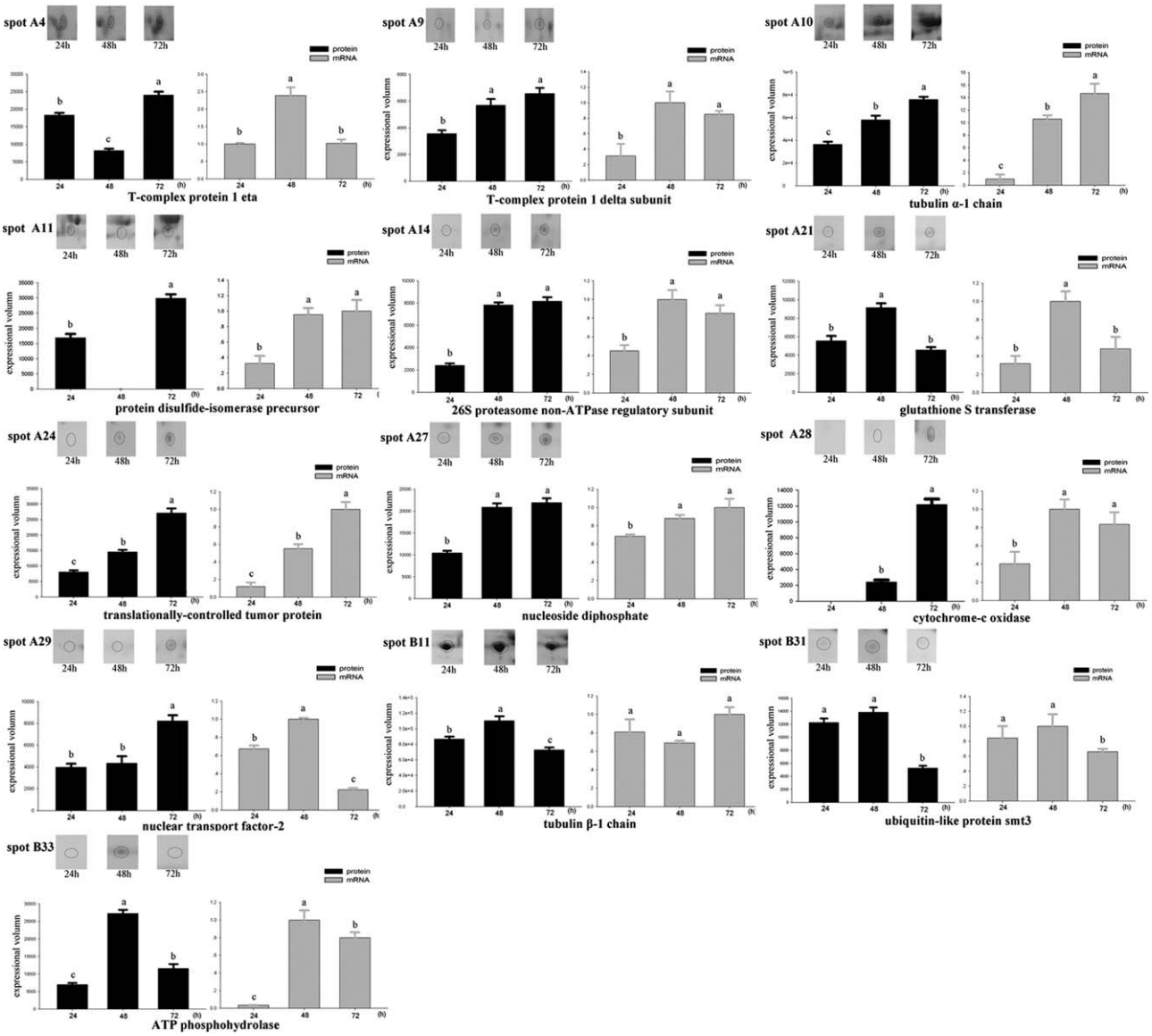

Fig. 5. Thirteen differentially expressed proteins occurring during the honeybee drone embryogenesis validated at mRNA level. The magnified images of protein spots from the 2-DE gels are shown in the upper part of each panel. The values of protein abundance are the average %vol of spots in three replicated gels. The lower case letters (a, b, c) above the lines indicate significant differences between day 1, day 2 and day 3 eggs ($p < 0.05$). (a) is significantly higher than (b) and (c), (b) is significantly higher than (c).

that function from early larva through pupa stages to adults. This is consistent with the knowledge that head and body segments are seen within the eggs by 72 h. The head is present at the larger unattached end while the back is on the incurved side (DuPraw, 1967; Winston, 1987).

The current identified cytoskeletal proteins were tubulin and actin. In *Drosophila*, actin plays an important role during dorsal closure throughout the embryonic development (Jacinto et al., 2002) and tubulin make up microtubules (MTs) (Tuszynsk, 2006). In the queen-right colony, workers showed signs of disorganized microtubule and microfilament system that could explain the histological evidence for progressive cell death observed in their germaria (Tanaka and Hartfelder, 2004). Several of cytoskeleton proteins and over expressed at 48 and 72 h is likely to ensure the developing embryos to maintain cell shape, motility, intracellular transportation and cellular division.

A complex network of antioxidant metabolites and enzymes such as catalase, superoxide dismutase and various peroxidases work together to prevent oxidative damage to cellular components and inhibit other oxidation reactions being oxidized themselves (Sies, 1997; Vertuani et al., 2004). In the honeybee genome, 38 antioxidant genes were annotated including all major components of the enzymatic antioxidant system (Corona, 2006). Expression of antioxidant genes generally increases in the younger queens (Corona, 2005). The high demand for oxygen during embryonic development leads to increased reactive oxygen species (ROS) production through increasing oxidative damage (Seehuus et al., 2006; Sies, 1997). Antioxidant proteins gsts1, sod, trxr-1, trx-2, dj-1β, thioredoxin peroxidase, sod, and peroxiredoxin-6 were identified in the current study. The up-regulation of gsts1 dj-1β and sod at 48 and 72 h, may play a role in the protection of embryos from ROS-mediated organ damage.

The nucleus is near the large end of the honeybee embryo egg. It has a critical role in the development of the future bee by nuclear division-if the egg is unfertilized, or the fusion of the nucleus and zygote division-if the egg is fertilized. In the present study these proteins were identified and found to be involved in the regulation of translation initiation and translation elongation. In *Drosophila*, Ntf-2 and PA2G4 are known to be associated with eye development, the immune response (Bhattacharya et

al., 2002), and embryonic muscle system formation (Takemori and Yamamoto, 2009). Up-regulation of PA2G4, eif2b, rplp0 and Ntf-2 at 48 or 72 h suggests likely roles played by these proteins in ensuring the fidelity of the multilayered process of encoding protein from DNA. The proteasome is a multi-catalytic proteinase complex which is characterized by its ability to cleave peptides with Arg, Phe, Tyr, Leu, and Glu adjacent to the leaving group at neutral or slightly basic pH. It has been reported that three proteasome subunits differ between ventralized and lateralized embryos in *Drosophila* and they have the roles in ventral furrow morphogenesis (Gong et al., 2004). In the present study, exclusive higher expression of amino acid metabolism proteins at 72 h suggests that the embryo requires more amino acid elements to facilitate its organogenesis preparing for larval life.

In the living cell most proteins act as integral parts of protein complexes rather than a single entity. Concurrent to this fact, we recognized 49 proteins that play a key role in the BIN (biological interaction network) of the mapped proteome of the honeybee drone embryos. Clearly, carbohydrate metabolism and energy production, development and protein folding related proteins played dominate roles in BIN. The visualized BIN enables us to target proteins for further functional confirmation.

qRT-PCR revealed that eight proteins exhibited a similar expression pattern at the transcription level but five other proteins did not. The inconsistent relationship between mRNA and protein expression may be due to the lack of a direct relationship between mRNA and protein expression, or unsynchronized gene transcription and translation. Understanding the relationship between gene transcription and translation will definitely facilitate gene manipulation which may help generate desirable phenotypes such as increased honey, pollen and royal jelly yields.

5. Conclusions

Our data generated a first preliminary proteome map of honeybee drone embryos. More than 100 proteins were successfully identified and 62 of them altered expressions at embryonic ages of 24, 48 and 72 h. A significant number of proteins were up-regulated at age 48 h, a peak time at which carbohydrate and energy metabolism-related proteins are required the most. Development and metabolizing amino acid-related proteins were expressed the greatest at embryonic age of 72 h. Protein involving in the cytoskeleton, antioxidants and protein folding were highly expressed at 48 and 72 h to maintain cell shape, or remove ROS or facilitate protein folding for the developing embryos. The constructed BIN and qRT-PCR validation results provide valuable information for geneticists to specify a precise embryonic age at which to select a suitable protein target for future manipulation of honeybee male stem cells for better pollination services or increased bee product yield.

Acknowledgements

I'm very grateful to Dr. John A. Kefuss, France, for their assistance in editing the manuscript. This work is supported by a special fund from the technical production system of the national beekeeping industry (NYCYTX-43); National Natural Science Foundation of China (No. 30972148) and the special scientific and research fund for the public welfare industry (nyhyzx07-041).

Appendix A. Supplementary data

Supplementary data associated with this article can be found, in the online version, at doi:10.1016/j.jinsphys.2010.12.007.

References

Aase, A.L.T.O., Amdam, G.V., Hagen, A., Omholt, S.W., 2005. A new method for rearing genetically manipulated honey bee workers. Apidologie 36, 293–299.
Amdam, G., Simoes, Z., Guidugli, K., Norberg, K., Omholt, S., 2003. Disruption of vitellogenin gene function in adult honeybees by intra-abdominal injection of double-stranded RNA. BMC Biotechnology 20, 1–3.
Amdam, G.V., Simoes, Z.L., Hagen, A., Norberg, K., Schroder, K., Mikkelsen, O., Kirkwood, T.B., Omholt, S.W., 2004. Hormonal control of the yolk precursor vitellogenin regulates immune function and longevity in honeybees. Experimental Gerontology 39, 767–773.
Baer, B., Eubel, H., Taylor, N.L., O'Toole, N., Millar, A.H., 2009. Insights into female sperm storage from the spermathecal fluid proteome of the honeybee *Apis mellifera*. Genome Biology 10, R67.
Bergem, M., Norberg, K., Aamodt, R., 2006. Long-term maintenance of in vitro cultured honeybee (*Apis mellifera*) embryonic cells. BMC Developmental Biology 6, 17.
Beye, M., Hasselmann, M., Fondrk, M.K., Page, R.E., Omholt, S.W., 2003. The gene csd is the primary signal for sexual development in the honeybee and encodes an SR-type protein. Cell 114, 419–429.
Bhattacharya, A., Muruganandam, A.V., Kumar, V., Bhattacharya, S.K., 2002. Effect of poly herbal formulation, EuMil, on neurochemical perturbations induced by chronic stress. Indian Journal of Experimental Biology 40, 1161–1163.
Borges, J.C., Ramos, C.H.I., 2005. Protein folding assisted by chaperones. Protein and Peptide Letters 12, 257–261.
Bradford, M.M., 1976. A rapid and sensitive method for the quantitation of microgram quantities of protein utilizing the principle of protein-dye binding. Analytical Biochemistry 72, 248–254.
Chan, Q.W., Foster, L.J., 2008. Changes in protein expression during honey bee larval development. Genome Biology 9, R156.
Chan, Q.W., Howes, C.G., Foster, L.J., 2006. Quantitative comparison of caste differences in honeybee hemolymph. Molecular and Cellular Proteomics 5, 2252–2262.
Collins, A., Williams, V., Evans, J., 2004. Sperm storage and antioxidative enzyme expression in the honey bee, *Apis mellifera*. Insect Molecular Biology 13, 141–146.
Corona, M., 2005. Gene expression patterns associated with queen honey bee longevity. Mechanisms of Ageing and Development 126.
Corona, M., 2006. Genes of the antioxidant system of the honey bee: annotation and phylogeny. Insect Molecular Biology 15.
De Maio, A., 1999. Heat shock proteins: facts, thoughts, and dreams. Shock 11, 1–12.
Dearden, P.K., 2006. Germ cell development in the honeybee (*Apis mellifera*); vasa and nanos expression. BMC Developmental Biology 6, 6.
DuPraw, E., 1967. The honeybee embryo. Methods in Developmental Biology 183–217.
Feng, M., Fang, Y., Li, J., 2009. Proteomic analysis of honeybee worker (*Apis mellifera*) hypopharyngeal gland development. BMC Genomics 10, 645.
Fleig, R., Sander, K., 1986. Embryogenesis of the honeybee *Apis mellifera* L. (Hymenoptera: Apidea): a SEM study. International Journal of Insect Morphology and Embryology 15, 449–462.
Garcia, L., Saraiva Garcia, C.H., Calabria, L.K., Costa Nunes da Cruz, G., Sanchez Puentes, A., Bao, S.N., Fontes, W., Ricart, C.A., Salmen Espindola, F., Valle de Sousa, M., 2009. Proteomic analysis of honey bee brain upon ontogenetic and behavioral development. Journal of Proteome Research 8, 1464–1473.
Gong, L., Puri, M., Unlu, M., Young, M., Robertson, K., Viswanathan, S., Krishnaswamy, A., Dowd, S.R., Minden, J.S., 2004. Drosophila ventral furrow morphogenesis: a proteomic analysis. Development 131, 643–656.
Gregorc, A., 1998. Histopathological and histochemical changes in honeybee larvae (*Apis mellifera* L.) after infection with Bacillus larvae, the causative agent of American foulbrood disease. Cell Biology International 22.
Gregorc, A., Bowen, I.D., 1999. In situ localization of heat-shock and histone proteins in honey-bee (*Apis mellifera* L.) larvae infected with Paenibacillus larvae. Cell Biology International 23, 211–218.
Hirsch, C., Gauss, R., Sommer, T., 2006. Coping with stress: cellular relaxation techniques. Trends in Cell Biology 16, 657–663.
Hrassnigg, N., Crailsheim, K., 2005. Differences in drone and worker physiology in honeybees (*Apis mellifera*). Apidologie 36, 255–277.
Hsu, Y.-C., Chern, J.J., Cai, Y., Liu, M., Choi, K.-W., 2007. Drosophila TCTP is essential for growth and proliferation through regulation of dRheb GTPase. Nature 445, 785–788.
Jacinto, A., Wood, W., Woolner, S., Hiley, C., Turner, L., Wilson, C., Martinez-Arias, A., Martin, P., 2002. Dynamic analysis of actin cable function during Drosophila dorsal closure. Current Biology 12, 1245–1250.
Javier, P.A., Havron, A., Morallo-Rejesus, B., Rosen, D., 1991. Selection for pesticide resistance in Aphytis. Entomologia Experimentalis et Applicata 61, 237–245.
Katanaev, V., 2006. Dual roles for the trimeric G protein Go in asymmetric cell division in Drosophila. Proceedings of the National Academy of Sciences of the United States of America 103.
Klenk, M., Koeniger, G., Koeniger, N., Fasold, H., 2004. Proteins in spermathecal gland secretion and spermathecal fluid and the properties of a 29 kDa protein in queens of *Apis mellifera*. Apidologie 35, 371–381.
Li, J., Li, H., Zhang, Z., Pan, Y., 2007. Identification of the proteome complement of high royal jelly producing bees (*Apis mellifera*) during worker larval development. Apidologie 38, 545–557.

Li, J., Zhang, L., Feng, M., Zhang, Z., Pan, Y., 2009. Identification of the proteome composition occurring during the course of embryonic development of bees (*Apis mellifera*). Insect Molecular Biology 18, 1–9.

Livak, K.J., Schmittgen, T.D., 2001. Analysis of relative gene expression data using real-time quantitative PCR and the 2(-Delta Delta C(T)) method. Methods 25, 402–408.

Molnar, C., Lopez-Varea, A., Hernandez, R., de Celis, J.F., 2006. A gain-of-function screen identifying genes required for vein formation in the *Drosophila melanogaster* wing. Genetics 174, 1635–1659.

Nelson, C.M., Ihle, K.E., Fondrk, M.K., Page, R.E., Amdam, G.V., 2007. The gene vitellogenin has multiple coordinating effects on social organization. PLoS Biology 5, e62.

Oron, E., 2002. COP9 signalosome subunits 4 and 5 regulate multiple pleiotropic pathways in *Drosophila melanogaster*. Development 129.

Peiren, N., de Graaf, D.C., Vanrobaeys, F., Danneels, E.L., Devreese, B., Van Beeumen, J., Jacobs, F.J., 2008. Proteomic analysis of the honey bee worker venom gland focusing on the mechanisms of protection against tissue damage. Toxicon 52, 72–83.

Seehuus, S.-C., Krekling, T., Amdam, G.V., 2006. Cellular senescence in honey bee brain is largely independent of chronological age. Experimental Gerontology 41, 1117–1125.

Sequencing Consortium, T.H.G., 2006. Insights into social insects from the genome of the honeybee *Apis mellifera*. Nature 444, 512–1512.

Severson, D.W., Erickson Jr., E.H., Williamson, J.L., Aiken, J.M., 1990. Heat stress induced enhancement of heat shock protein gene activity in the honey bee (*Apis mellifera*). Experientia 46, 737–739.

Sies, H., 1997. Oxidative stress: oxidants and antioxidants. Experimental Physiology 82, 291–295.

Silva-Zacarin, E.C.M., Gregorc, A., Moraes, R.L.M.S.d., 2006. In situ localization of heat-shock proteins and cell death labelling in the salivary gland of acaricide-treated honeybee larvae. Apidologie 37, 507–516.

Takemori, N., Yamamoto, M.T., 2009. Proteome mapping of the *Drosophila melanogaster* male reproductive system. Proteomics 9, 2484–2493.

Talamillo, A., Sanchez, J., Cantera, R., Perez, C., Martin, D., Caminero, E., Barrio, R., 2008. Smt3 is required for *Drosophila melanogaster* metamorphosis. Development 135, 1659–1668.

Tanaka, E.D., Hartfelder, K., 2004. The initial stages of oogenesis and their relation to differential fertility in the honey bee (*Apis mellifera*) castes. Arthropod Structure & Development 33, 431–442.

Tuszynsk, J., 2006. The evolution of the structure of tubulin and its potential consequences for the role and function of microtubules in cells and embryos. International Journal of Developmental Biology 50.

Vertuani, S., Angusti, A., Manfredini, S., 2004. The antioxidants and pro-antioxidants network: an overview. Current Pharmaceutical Design 10, 1677–1694.

Winston, M.L., 1987. The Biology of the Honey Bee. Harvard University Press, Cambridge, London.

Woolworth, J.A., Nallamothu, G., Hsu, T., 2009. The *Drosophila metastasis* suppressor gene Nm23 homolog, awd, regulates epithelial integrity during oogenesis. Molecular and Cellular Proteomics 29, 4679–4690.

Xu, J., Liu, L.Z., Deng, X.F., Timmons, L., Hersperger, E., Steeg, P.S., Veron, M., Shearn, A., 1996. The enzymatic activity of Drosophila AWD/NDP kinase is necessary but not sufficient for its biological function. Developmental Biology 177, 544–557.

Zeng, Z., Huang, Z.Y., Qin, Y., Pang, H., 2005. Hemolymph juvenile hormone titers in worker honey bees under normal and preswarming conditions. Journal of Economic Entomology 98, 274–278.